Bull. Mater. Sci. (2018) 41:105
https://doi.org/10.1007/s12034-018-1617-z

Effect of annealing on tungsten oxide thin films for acetone gas detection

SMITI SACHDEVA[1,2,*], RAVINDER AGARWAL[1] and AJAY AGARWAL[2]
[1]Thapar University, Patiala 147001, India
[2]CSIR – Central Electronics Engineering Research Institute, Pilani 333031, India
*Author for correspondence (ssmiti27@gmail.com)

MS received 26 July 2017; accepted 30 November 2017; published online 26 July 2018

Abstract. The gas-sensing properties and topology of tungsten oxide thin films deposited by reactive-ion radiofrequency magnetron sputtering were investigated at room temperature. The abnormalities in sensing film behaviour were observed when acetone gas is flowed over surface. The reduction reaction of surface and oxidation reaction of acetone gas were studied. As the gas comes in contact with the surface, the molecules tend to reduce the surface, hence, decreasing the resistance. The sensing film was annealed at different temperatures, viz., 300, 400, 500, 600 and 700°C for 1 h each for the purpose of finding the optimum annealing temperature to detect acetone gas. Various characterizations, viz., XRD, AFM, FESEM, thickness measurement through surface profiler, gas-sensing characterization for recording resistance changes were performed. The optimum annealing temperature at which the sensing film gives maximum response when it comes in contact with acetone gas was computed to be 500°C. Also, operational optimum temperature for sensing film annealed at 500°C was computed to be 260°C. A grain size of 7.3 nm was computed through analysis of AFM image and a film thickness of 100 nm was calculated through surface profiler. The SEM image of the film demonstrates that the grains developed on the surface, which increase in size with increase in the annealing temperature. The XRD patterns reveal that the oxide showed up was WO_2. It was observed that the response percentage is ∼31% for acetone vapour concentration of 20 ppm, ∼19% for the concentration of 15 ppm and ∼15% for the concentration of 10 ppm. The response time of the sensor is ∼5 min and the recovery time is 4 min.

Keywords. Tungsten oxide thin films; gas sensing; acetone gas detection; optimum annealing temperature.

1. Introduction

Tungsten oxide is a very important semiconductor material. This wide gap semiconductor has played a vital role in numerous areas, viz., optical modulation devices, flat panel displays, gas sensors, humidity and temperature sensors, etc. [1]. The naturally occurring n-type semiconductor was found to have great application as a metal oxide-based gas sensor [2], electrochromic device [3], humidity sensor [4], etc. Several distinct structures, like nanopowders [5], nanorods [6,7], nanoplatelets, nanoparticles, nanowires [8], thin films [9–11], were brought forward for gas-sensing applications of tungsten oxide. Tungsten oxide can be formed by various methods, viz., sputtering [12], chemical vapour deposition [13], sol–gel [14], thermal evaporation [15,16] and spray pyrolysis [17]. This study focusses on the acetone gas-sensing properties of reactively sputtered tungsten oxide thin films. Most of the methods used for tungsten oxide formation require post-annealing to achieve optimized parameters for the purpose of gas sensing. Most of these studies are focussed on tungsten trioxide, while other non-stoichiometric forms were not extensively studied.

The tungsten–oxygen (W–O) system described the various regions of tungsten oxide, viz., α-W, WO_2, $W_{18}O_{49}$, $W_{24}O_{68}$, W_nO_{3n-1} and WO_3. It was also reported that with increase in temperature from −143 to 1474°C, WO_3 occurs in various forms, namely monoclinic, triclinic, orthorhombic and tetragonal. In addition to this, βW is not a stable phase and is not the W_3O oxide [18]. Tungsten dioxide or wolfram dioxide was one of the first tungsten oxides to be recognized [19]. WO_2 is known to have distorted octahedral WO_6 centres with alternate short W–W bond (248 pm) [20]. Also, in the temperature range of −200 to 1527°C, no phase changes were observed [22]. Similarly, no phase change was detected in the range 67–717°C [23]. The current study is focussed on WO_2 and the grains developed, while the sputtered thin film is annealed at different temperatures.

Grain size plays an important role in computation of conductivity of the sensing film. The conductivity of the thin film can be estimated through the relation $\sigma = A[C]^N$, where A is a constant, C the concentration of gas to be tested and N varies between 0.5 and 1, depending on the grain size. The grain size is nearly equal to $2L_D$, where L_D is the width of the depletion layer [24]. For a very small grain size ($D << 2L_D$), crystallites are depleted of mobile charge carriers as the depletion layer is extended throughout the whole grain. As a consequence, the conductivity declines sharply

since the conduction channels between the grains will vanish. In the case of $D \geq 2L_D$, the depletion region around each neck forms a constricted conduction channel within each aggregate [25,26].

The emission of acetone gas, which is widely used in industrial applications, is harmful to human health. In various studies, concentrations of 300–500 ppm were reported to cause irritation of eyes, throat, lungs and nose. With an exposure of around 250 ppm for 4 h, slight effects in performance of some behavioural tests, like mood test and auditory test were observed. As the concentration approaches 1000 ppm, one can experience dizziness, confusion and unsteadiness. Even higher concentrations of 2000 ppm can even cause drowsiness, vomiting and nausea. Further higher concentrations can lead to collapse, coma and even death [27].

Apart from the use in industrial applications, acetone was proven to be a biomarker for diabetes [28]. Breath analysis has attracted many researchers because of its numerous advantages, viz. sample collection is an easy task, breath is a less complex mixture in comparison to other fluids available in the body such as urine or blood, etc. [29]. Acetone, the biomarker for type I diabetes, was considerably in low concentration in human breath. For a healthy individual, the concentration ranges from 0.22 to 0.80 ppm, whereas for a person suffering from diabetes, it exceeds 1.8 ppm [30–32].

The aim of this study is to study the evolution of structural changes in thin film of tungsten oxide (WO_2) as a function of annealing and its acetone gas detection ability.

2. Materials and methods

2.1 *Preparation of film*

After standard cleaning procedures of n-type silicon wafers, silicon dioxide was thermally grown as an electrical isolation layer with a thickness of 1 μm. Tungsten oxide thin films were deposited by reactive-ion sputtering at room temperature maintaining a ratio of 80:20% of argon and oxygen gas, respectively. The flow rates of argon and oxygen gas were set as 32 and 8 ccm, respectively, so as to maintain a ratio of 80:20%. The chamber pressure was maintained at 3 mTorr and the distance between target metal and silicon dioxide sample was set to 15 cm. The process was optimized so as to achieve the thickness of 100 nm. The fabricated devices were diced with a size of 5 mm × 5 mm. The chips were wire bonded with epoxy at two points to carry on the gas-sensing procedure. These chips were then annealed in ambient air in a chamber at elevated temperatures of 300, 400, 500, 600 and 700°C for 1 h each.

2.2 *Characterization of film*

The topography of sensing film was characterized using atomic force microscopy (AFM). The measurements were performed after the deposition process. The thickness of thin film was measured using a surface profiler. The crystallinity was determined using X-ray diffraction (XRD) method. X-ray diffractometer with copper target and Kβ radiation (λ = 1.39225 Å) was used, where the diffracted X-ray intensities were recorded as a function of 2θ. The sample was scanned from 20 to 90° (2θ) in steps of 0.02°. The imaging of the samples was performed using field emission scanning electron microscopy (FESEM).

The gas-sensing characterization for acetone gas was performed using the setup shown in figure 1. The components of the setup include computerized gas mixer, gas-testing chamber, computer for monitoring the changes in resistance of sensing film, digital multimeter and power supply.

2.3 *Gas concentration calculations*

The tungsten oxide thin film device was kept in the gas-sensing chamber (as shown in figure 1). The base of this gas-sensing chamber was heated at an optimum temperature of 260°C. The semiconductor films work at a particular temperature, i.e., the surface reactions between the sensing film and the gas to be sensed, take place at an optimum temperature. Initially, the chamber was flushed with dry air and the resistance of the thin film was allowed to stabilize.

Figure 1. Gas-sensing setup for detection of acetone gas.

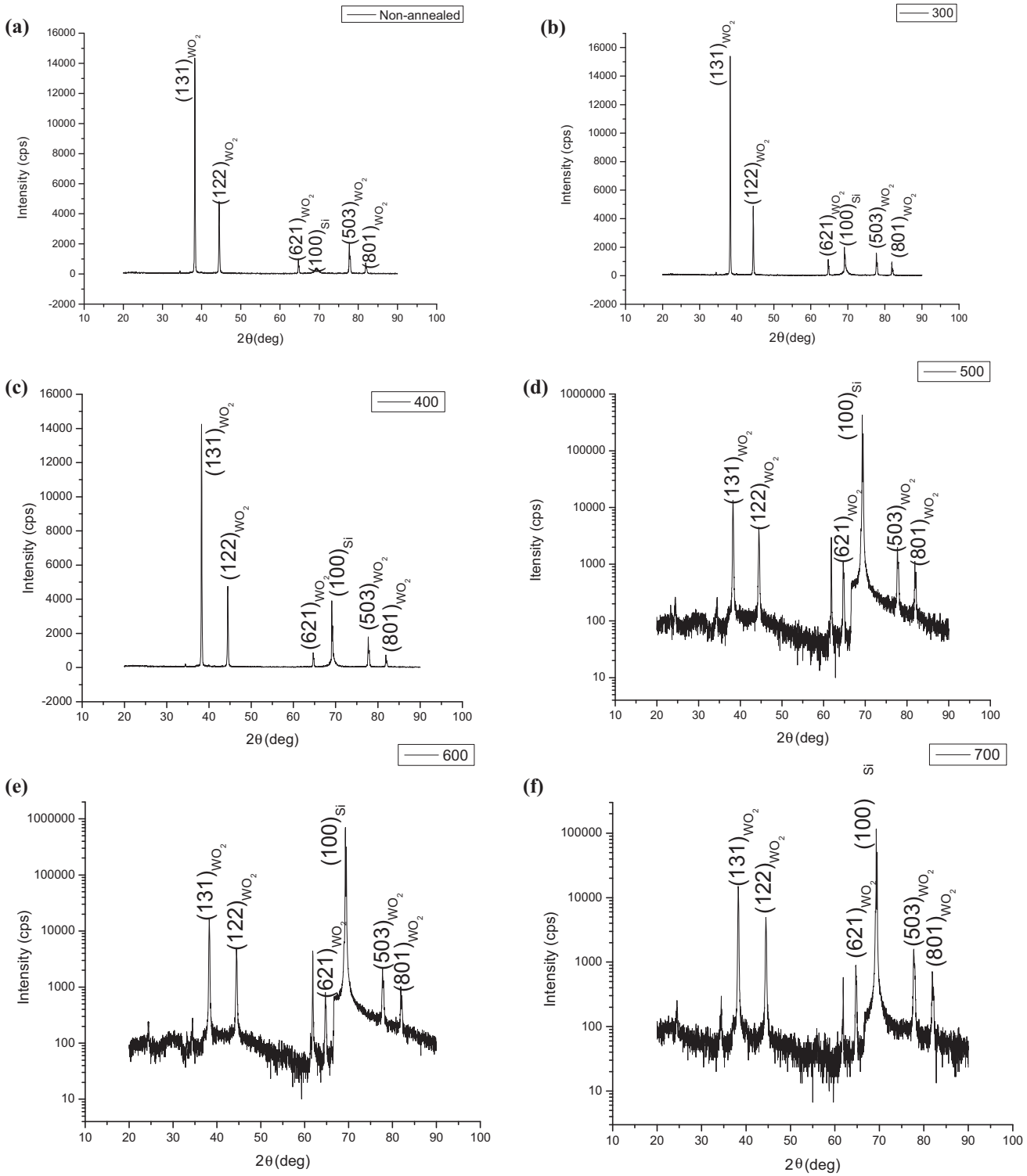

Figure 2. XRD pattern for (**a**) as-deposited tungsten oxide (WO_2) thin film and annealed at (**b**) 300, (**c**) 400, (**d**) 500, (**e**) 600 and (**f**) 700°C (ICSD PDF #820728).

Once the resistance of tungsten oxide thin film was stabilized, the chamber was flushed with acetone gas and the response was calculated using the formula $S = (R_f - R_i) \times 100/R_i$, where R_f is the final resistance obtained after the reaction with gas and R_i the initial resistance when the sensing film is in the presence of air. Different concentrations of acetone gas were introduced on the chamber and the response was calculated. The concentration is calculated by considering the flow

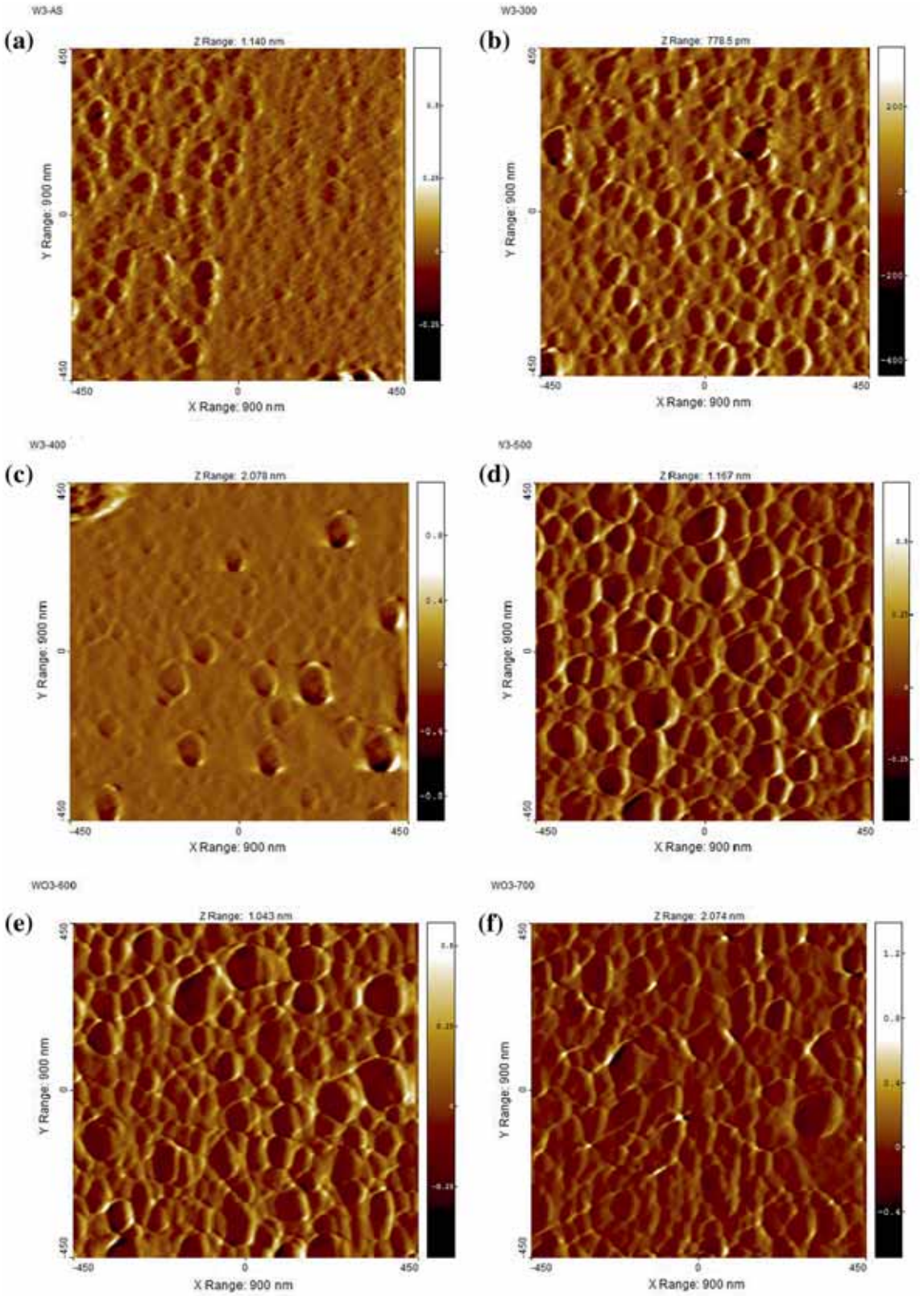

Figure 3. Atomic force microscopy images of sensing film for (**a**) as-deposited tungsten oxide (WO_2) thin film and annealed at (**b**) 300, (**c**) 400, (**d**) 500, (**e**) 600 and (**f**) 700°C. (a) Grain size: 4 nm, roughness: 0.0356 nm; (b) grain size: 8.1 nm, roughness: 0.0604 nm; (c) grain size: 9.5 nm, roughness: 0.0519 nm; (d) grain size: 7.3 nm, roughness: 0.1169 nm; (e) grain size: 6.6 nm, roughness: 0.1074 nm; (f) grain size: 6.5 nm, roughness: 0.0930 nm.

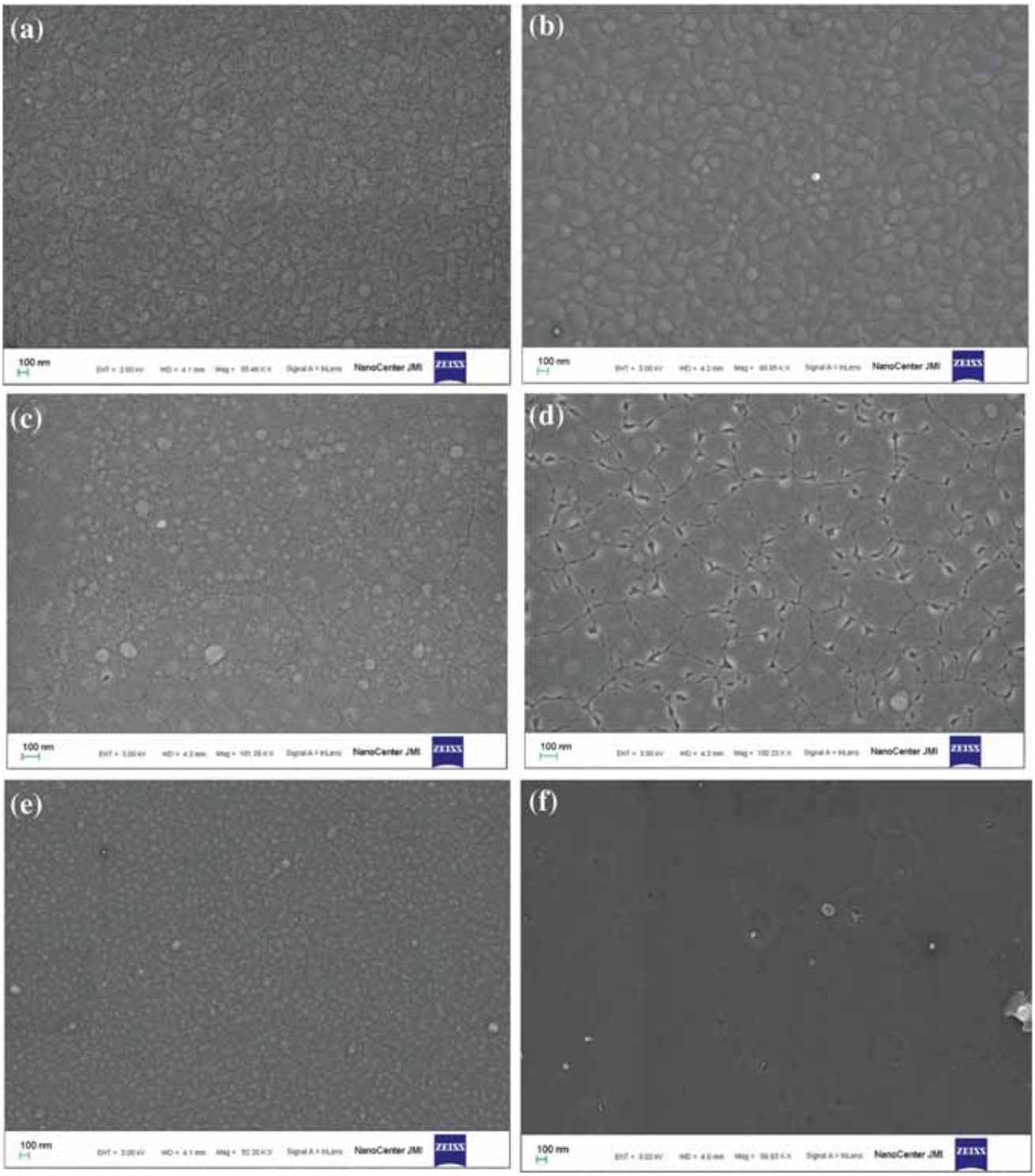

Figure 4. SEM images of sensing film for (**a**) as-deposited tungsten oxide (WO_2) thin film and annealed at (**b**) 300, (**c**) 400, (**d**) 500, (**e**) 600 and (**f**) 700°C.

rates of dry air and acetone gas. The method to calculate the concentration is described as follows:

Flow rate of acetone gas, x = 12 ccm,

Flow rate of dry air, y = 288 ccm.

Therefore,

Total flow rate = $x + y = t$ = 12 ccm + 288 ccm = 300 ccm,

Volume % of gas = $x/(x + y) \times 100 = (x/t \times 100) = 12/(12 + 288) \times 100 = 4\%$.

Concentration of acetone gas cylinder at which it is filled = 500 ppm.

Therefore,

Concentration of acetone gas = 4% of 500 ppm = $(4/100) \times 500 = 20$ ppm.

It can be stated as follows:

Required concentration (ppm) = Volume fraction × Concentration of cylinder (ppm).

Hence, if the flow rates are known, the required concentration of acetone gas can be computed. For example:

required concentration of acetone gas = 20 ppm,

concentration of cylinder = 500 ppm,

Total flow, t = 300 ccm.

Therefore, by using the formula:

Required concentration (ppm) = Volume fraction × Concentration of cylinder (ppm),

i.e., $20 = x/t \times 500$,

i.e., $20 = x/300 \times 500$.

Hence, $x = 12$ ccm and $y = t - x$ = 500 ccm − 12 ccm = 288 ccm.

Therefore, it is concluded that by setting these flow rates of acetone gas and dry air, the concentration of acetone gas can be computed.

3. Results and discussion

The film thickness was computed as nearly 1000 Å, i.e., 100 nanometres using the DEKTAK surface profiler. The XRD patterns depicted in figure 2 reveal the formation of orthorhombic phase of tungsten oxide. The XRD pattern (figure 2) of the thin film indicated reflections of WO_2 (ICSD PDF #820728) with average cell parameters: a = 9.716 Å, b = 8.438 Å, c = 4.756 Å.

The AFM measurements (figure 3) were further carried out to monitor the changes in surface morphology of the thin film. With increase in the annealing temperature, it was observed that the grain size was increased, giving rise to larger crystallites. The grain size varied from 4 to 6.5 nm. The evolution of the grain size as a function of annealing is shown in figure 4. The roughness of the film also varied from 0.0356 to 0.0930 nm. Roughness plays an essential role, while sensing the target gas. It was depicted that surface roughness enhances film sensitivity towards the target gas [33]. Many researchers have drawn their attention to the roughness of the thin film to enhance the sensitivity [34,35].

The samples annealed at different temperatures were viewed through scanning electron microscope (SEM) and distinguishable grain boundaries were observed. The SEM images in figure 4 reveal that with increase in the temperature at which the thin films are annealed, grains size increases from 300 to 700°C.

Each annealed sample was tested for its capability of detecting acetone gas. It was observed that the maximum response was observed at tungsten oxide film annealed at 500°C, i.e., 30% for 20 ppm of acetone towards tungsten oxide thin film. Hence, the optimized annealing temperature was computed as 500°C as shown in figure 5. It can be stated that a grain size of 7.3 nm was observed as an optimized value for sensing acetone gas. Grain size plays an important role in the computation of conductivity. An optimum grain size is required to have proper gas sensing and reactions between the substrate and the gas molecules. The semiconductor films work at a particular temperature, i.e., the surface reactions between the sensing film and the gas to be sensed take place at an optimum temperature. Response percentage at different temperatures was computed so as to discover the optimum temperature. The response was calculated using the formula $S = (R_f - R_i) \times 100/R_i$, where R_f is the final resistance obtained after the reaction with gas and R_i is the initial resistance when the sensing film is in the presence of air. Figure 6 shows the graph for optimum temperature, which was computed as 260°C.

The sensing film creates oxygen ion species O^- and O^{2-} when in air, i.e., the WO_2 film interacts with the oxygen, by transferring the electrons from the conduction band to adsorbed oxygen atoms, resulting into the formation of ionic species such as O^{2-} or O^-.

$$O_2 \text{ (gas)} \longleftrightarrow O_2 \text{ (adsorbed)},$$

$$O_2 \text{ (adsorbed)} + e^- \longleftrightarrow O_2^-,$$

$$O_2^- + e^- \longleftrightarrow 2O^-.$$

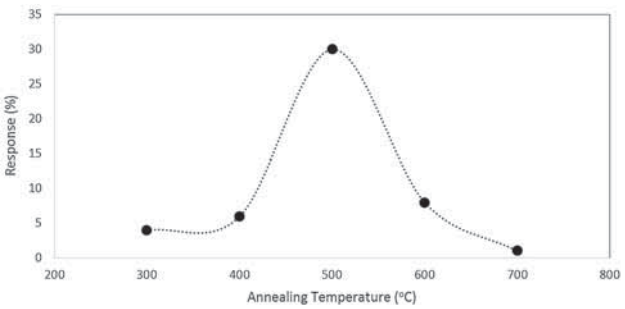

Figure 5. Optimum annealing temperature.

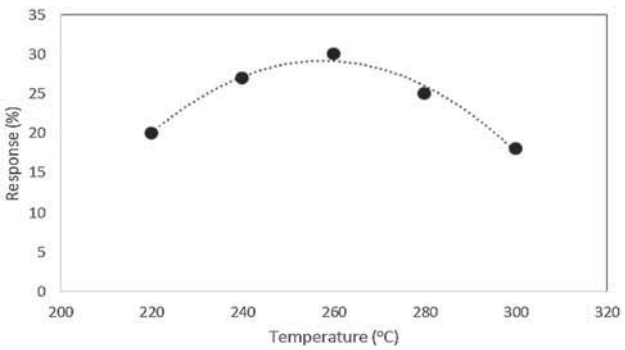

Figure 6. Plot for calculation of optimum temperature at which sensing film operates efficiently.

The electron transfer from the conduction band to the chemisorbed oxygen results in the decrease in electron concentration of the film. As a consequence, an increase in the resistance of the tungsten oxide film is observed. When the sensing film is exposed to reducing gas like acetone, the acetone vapour reacts with the chemisorbed oxygen releasing an electron back to the conduction band, which decreases the resistance of the tungsten oxide film [35].

$$CH_3COCH_3\ (gas) + OH^- \rightarrow CH_3CHO + CH_3O^-,$$
$$CH_3COCH_3\ (gas) + O^- \rightarrow CH_3COC^+H_2 + OH^- + e^-,$$
$$CH_3CHO + O\ (bulk) \rightarrow CH_3COOH + O\ (vacancies),$$

or

$$CH_3COCH_3\ (gas) + O^- \rightarrow CH_3C^+O + CH_3O^- + e^-,$$
$$CH_3C^+O \rightarrow C^+H_3 + CO,$$
$$CO + O^- \rightarrow CO_2 + e^-.$$

Time *vs.* resistance plots were constructed to observe the response of acetone over WO_2 sensing film. Different concentration levels were tested as shown in figures 7, 8 and 9.

It was observed that the response percentage is ∼31% for acetone vapour concentration of 20 ppm, ∼19% for the concentration of 15 ppm and ∼15% for the concentration of 10 ppm. The response time of the sensor is ∼5 min and the recovery time is 4 min. The shelf life of this sensor is ∼1 month. The repeatability of the sensor is 0.577, which means that the majority of response measurements of acetone gas are expected to be within 0.577 of the stated response percentage in the text.

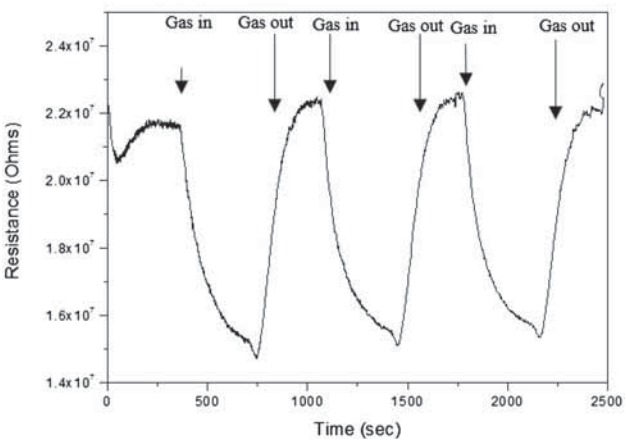

Figure 7. Resistance changes in sensing film when exposed to 20 ppm of acetone at 260°C for a particular time interval. Three cycles of exposure, which are turned on and off as shown.

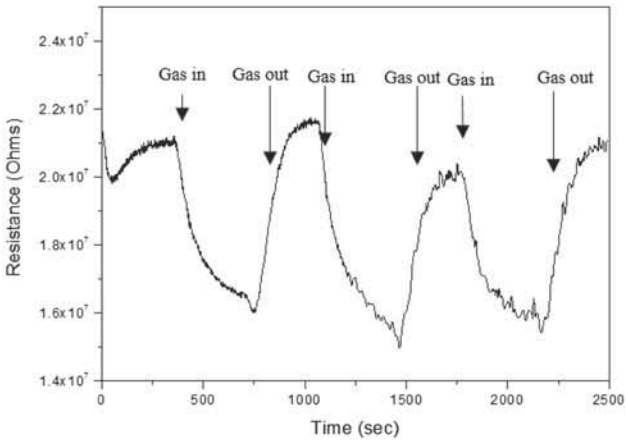

Figure 8. Resistance changes in sensing film when exposed to 15 ppm of acetone at 260°C for a particular time interval. Three cycles of exposure, which are turned on and off as shown.

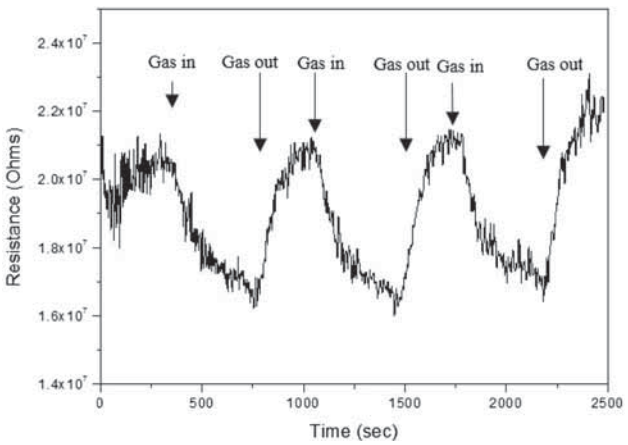

Figure 9. Resistance changes in sensing film when exposed to 10 ppm of acetone at 260°C for a particular time interval. Three cycles of exposure, which are turned on and off as shown.

4. Conclusion

Tungsten oxide was proven to be a great metal oxide material for gas-sensing applications. Characterization of such important material gives a glimpse of its gas-sensing properties. The process of annealing the tungsten oxide film at an elevated temperature of 500°C gave rise to formation of grains with a mean grain size of 7.3 nm. Grain size plays an important role in computation of conductivity. Tungsten oxide thin films were annealed at different temperatures ranging from 300 to 700°C and an increase in grain size was observed with increase in annealing temperature. Various characterizations, viz., XRD, AFM and SEM were performed to observe the changes in topography of the film. This work was focussed towards sensing of acetone gas through a thin film of tungsten oxide. Gas sensing is a complex surface chemistry process. The sensing film of metal oxide develops oxygen ions on its surface. These oxygen ion species trap the electrons present

in the conduction band of the metal oxide, thus, increasing its resistance. When a reducing gas such as acetone strikes the surface, it forms compounds with the oxygen ion species present on the surface, giving back the electrons to the conduction band of metal oxide. This reduces the resistance of the sensing film. Same phenomenon was observed when acetone comes in contact with the surface of tungsten oxide. Two different concentrations of the same were depicted. The response percentage is ∼31% for 20 ppm, ∼19% for 15 ppm and ∼15% for 10 ppm of acetone vapour concentrations at an optimum operational temperature of 260°C.

Acknowledgements

We are thankful to Dr Prakash Gopalan, Director, Thapar University, Patiala and Prof Santanu Chaudhury, Director, CSIR-CEERI, Pilani, for providing the research facilities. Financial support provided by Department of Science and Technology (DST-INSPIRE Fellowship), New Delhi, Govt. of India, is gratefully acknowledged.

References

[1] Li X L, Lou T J, Sun X M and Li Y D 2004 *Inorg. Chem.* **43** 5442
[2] Penza M, Tagliente M A, Mirenghi L, Gerardi C, Martucci C and Cassano G 1998 *Sens. Actuator B-Chem.* **50** 9
[3] Granqvist C G 2003 *Sol. Energ. Mat. Sol. Cells* **60** 201
[4] Zhang J, Zhang W, Yang Z, Yu Z, Zhang X, Chang T C *et al* 2014 *Sens. Actuator B-Chem.* **202** 708
[5] Jimenez I, Arbiol J, Dezanneau G, Cornet A and Morante J R 2003 *Sens. Actuator B-Chem.* **93** 475
[6] Jia Q Q, Ji H M, Wang D H, Bai X, Sun X H and Jin Z G 2014 *J. Mater. Chem. A* **2** 13602
[7] Liu Z, Miyauchi M, Yamazaki T and Shen Y 2009 *Sens. Actuator B-Chem.* **140** 514
[8] Rout C S, Hegde M and Rao C N R 2008 *Sens. Actuator B-Chem.* **128** 488
[9] Tamaki J, Hayashi A, Yamamoto Y and Matsuoka M 2003 *Sens. Actuator B-Chem.* **95** 111
[10] Aguir K, Lemire C and Lollman D B B 2002 *Sens. Actuator B-Chem.* **84** 1
[11] Cantalini C, Sun H T, Faccio M, Pelino M, Santucci S, Lozzi L *et al* 1996 *Sens. Actuator B-Chem.* **31** 81
[12] Monteiro A, Costa M F, Almeida B, Teixeira V, Gago J and Roman E 2002 *Vacuum* **64** 287
[13] Kuypers A D, Spee C I M A, Linden J L, Kirchner G, Forsyth J F and Mackor A 1995 *Surf. Coat Technol.* **74** 1033
[14] Tong M, Dai G and Gao D 2001 *Mater. Chem. Phys.* **69** 176
[15] Penza M, Cassano G and Tortorella F 2001 *Sens. Actuator B-Chem.* **81** 115
[16] Lozzi L, Ottaviano L, Passacantando M, Santucci S and Cantalini C 2001 *Thin Solid Films* **391** 224
[17] Regragui M, Jousseaume V, Addou M, Outzourhit A, Bernede J C and El Idrissi B 2001 *Thin Solid Films* **397** 238
[18] Wriedt H A 1989 *Bull. Alloy Phase Diagr.* **10** 368
[19] Desi E D 1897 *J. Am. Chem. Soc.* **19** 213
[20] Wells A F 2012 *Structural inorganic chemistry* (5th ed.) (Oxford: Clarendon Press)
[21] King E G, Weller W W and Christensen A U 1960 *Bureau of mines* BM-RI-5664
[22] Sale F R 1979 *Thermochim Acta* **30** 163
[23] Ogawa H, Nishikawa M and Abe A 1982 *J. Appl. Phys.* **53** 4448
[24] Rout C S, Hegde M, Govindaraj A and Rao C N R 2007 *Nanotechnology* **18** 205504
[25] Tamvakos A, Calestani D, Tamvakos D, Mosca R, Pullini D and Pruna A 2015 *Microchimica Acta* **182** 1991
[26] Liu S, Zhang F, Li H, Chen T and Wang Y 2012 *Sens. Actuator B-Chem.* **162** 259
[27] Kao K W, Hsu M C, Chang Y H, Gwo S and Yeh J A 2012 *Sensors* **12** 7157
[28] Manolis A 1983 *Clin. Chem.* **29** 5
[29] Minh T D C, Blake D R and Galassetti P R 2012 *Diabetes Res. Clin. Pract.* **97** 195
[30] Righettoni M and Tricoli A 2011 *J. Breath Res.* **5** 037109
[31] Righettoni M, Tricoli A and Pratsinis S E 2010 *Anal. Chem.* **82** 3581
[32] Durrani S, Al-Kuhaili M F, Bakhtiari I A and Haider M B 2012 *Sensors* **12** 2598
[33] Ziabari A A, Rozati S M, Bargbidi Z and Kiriakidis G 2012 *Trans. Electr. Electron. Mater.* **13** 111
[34] Zakrzewska K 2001 *Thin solid films* **391** 229
[35] Khadayate R S, Sali J V and Patil P P 2007 *Talanta* **72** 1077